

# Atlas-Based Segmentation of Brain Tumor Images Using a Markov Random Field-Based Tumor Growth Model and Non-Rigid Registration

Stefan Bauer, Christof Seiler, Thibaut Bardyn, Philippe Buechler and Mauricio Reyes

**Abstract**—We propose a new and clinically oriented approach to perform atlas-based segmentation of brain tumor images. A mesh-free method is used to model tumor-induced soft tissue deformations in a healthy brain atlas image with subsequent registration of the modified atlas to a pathologic patient image. The atlas is seeded with a tumor position prior and tumor growth simulating the tumor mass effect is performed with the aim of improving the registration accuracy in case of patients with space-occupying lesions. We perform tests on 2D axial slices of five different patient data sets and show that the approach gives good results for the segmentation of white matter, grey matter, cerebrospinal fluid and the tumor.

## I. INTRODUCTION

Accurate automatic segmentation of important brain structures from Magnetic Resonance Imaging (MRI) is of major interest for surgical planning procedures as well as for physiological and biomechanical modeling. Atlas-based segmentation of different tissue types like grey matter (GM), white matter (WM) and cerebrospinal fluid (CSF) is an established way to classify different tissues in MR images of healthy humans [1]. The different atlas tissue labels are propagated to the patient image through warping with a deformation field obtained by non-rigid registration techniques. However, this strategy fails in case of brain tumor images because of the missing tumor prior in the atlas.

Several groups [2], [3], [4] suggest to circumvent this problem by introducing a tumor seed into the atlas and grow the tumor to its approximate shape using different methods. Cuadra et al. [2] use a model of lesion growth which does not consider any mechanical tissue properties, while Mohamed et al. [3] use a finite element method (FEM) model to calculate tissue displacements induced by the tumor mass effect according to the mechanical properties of the surrounding tissues. After introducing a tumor prior into the atlas, this modified atlas image is warped to the patient image using non-rigid registration algorithms, thus implicitly performing segmentation. A good overview of the state of the art was collected by Angelini et al. in [5].

It is clearly desirable to incorporate mechanical tissue properties into models of tumor-induced deformations. FEM-based methods offer this capability, however they suffer from the need of transforming the data into a mesh. Automatic mesh generation is a challenging and error-prone task, while semi-automatic mesh generation is tedious and time-consuming. Additionally, large-scale deformations of the mesh are difficult to handle. Therefore, a completely

image-processing based method, which does not require any meshing would greatly simplify this task. Such an approach is suggested in [4], but it suffers from difficult parameterization and for reasons of computation speed it runs on a subsampled version of the input image only, which hinders its clinical usability.

Our aim is to develop a simple tool to segment brain tissues based on previous segmentation of the tumor areas. While tumor segmentation can be done manually or using (semi)-automatic methods with reasonable effort, the segmentation of brain tissues is a time-consuming and tedious task. However, tissue segmentation is necessary in order to be able to apply more sophisticated models to simulate and predict patient-specific tumor progression. The tool should be sufficiently simple and generally applicable to be used by clinicians without expert knowledge in model parameterization on a daily basis.

## II. MATERIALS & METHODS

We show the application of a clinically-oriented, mesh-free method for modeling soft-tissue deformations to tumor-induced deformation and segmentation of pathologic brain images. It is based on finite differences in a local neighborhood of each voxel using Markov Random Fields (MRF). The work was initially proposed in [6] and validated against an FEM-based deformation method with good results on a number of synthetic cases. In this work it was adopted to account for deformations in pathological brain images and is briefly described in the next section.

### A. Hierarchical Displacement Model

The general idea outlined by Seiler et al. in [6] is to minimize an energy function

$$U_{\text{total}} = U_{\text{prior}} + U_{\text{observation}} \quad (1)$$

where  $U_{\text{prior}}$  represents the biomechanical information of the brain tissues and  $U_{\text{observation}}$  introduces boundary conditions. These energies are minimized in cliques of a neighborhood system surrounding a center voxel. Local tissue characteristics are based on Young's modulus. Four exemplary cliques of one center voxel  $t$  are shown in Fig. 1.

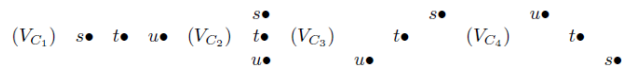


Fig. 1. Four different cliques belonging to the center voxel  $t$  in 2D.

S. Bauer, C. Seiler, T. Bardyn, P. Buechler and M. Reyes are with the Institute of Surgical Technology and Biomechanics, University of Bern, Switzerland; e-mail: stefan.bauer@istb.unibe.ch

For each clique  $C_i$ , the prior energy is calculated at each voxel  $t$  as

$$V_{pC_i} = \left| \frac{m_t}{m_u} (\mathbf{d}_t - \mathbf{d}_s) - (\mathbf{d}_u - \mathbf{d}_t) \right|^2 + \left| \frac{m_t}{m_s} (\mathbf{d}_t - \mathbf{d}_u) - (\mathbf{d}_s - \mathbf{d}_t) \right|^2. \quad (2)$$

Equation 2 uses a linear model, where  $m_{\{s,u,t\}}$  represents the material properties of the different tissues and  $\mathbf{d}_x$  is a displacement vector. The overall prior energy is obtained by summing over all cliques  $C_i$  at each voxel  $t$  in the complete image region  $\Omega$

$$U_{prior} = \sum_{t \in \Omega} \sum_i V_{pC_i}. \quad (3)$$

The observation energy is also calculated at each voxel as

$$V_{oC_i} = p_{\mathbf{x}_s} | \mathbf{b}_{\mathbf{x}_s} - \mathbf{d}_{\mathbf{x}_s} |. \quad (4)$$

$p_{\mathbf{x}_s}$  is a penalty term which is only non-zero at voxels where boundary conditions should be applied,  $\mathbf{b}_{\mathbf{x}_s}$  is the boundary condition vector, and  $\mathbf{d}_{\mathbf{x}_s}$  the displacement vector at position  $\mathbf{x}_s$ . The overall observation energy for the complete image can be calculated as

$$U_{observation} = \sum_{t \in \Omega} \sum_i V_{oC_i}. \quad (5)$$

In order to be able to use fast and stable local optimizers, the image is processed in a hierarchical way, resulting in a hierarchical Markov Random Fields (HMRf) approach. Iterative Conditional Modes (ICM) is used as a local optimizer at each level of hierarchy in order to find the best solution. This solution is used as an initial guess for the initialization of the next level.

### B. Application to Tumor Growth Modeling

The mass effect of a brain tumor is simulated using the above mentioned model. In this study we concentrate on the tumor mass effect since it has the largest impact on the deformation. The tumor is grown from a small circular seed. Inside the tumor an outward-pushing force is applied, modeled as a displacement field, which deforms the surrounding tissues according to the assigned mechanical properties.

The outward pushing force is assumed to be radial, which is accepted as good approximation for glioma growth [2]. However, this radial force does not restrict the tumor to a circular shape as the final shape is determined by the properties of the surrounding tissues and not only by the deformation field of the tumor. In order to circumvent warping problems in case of large deformations, the growth is performed in an iterative way until the approximate patient tumor volume and shape is attained. Thus, the hierarchical displacement model presented in section II-A is applied iteratively, simulating a small displacement at each step. The growth displacement field is employed in a narrow band of 3 voxels around the

tumor boundary. This leads to better control of the tumor growth behavior and can also be physiologically justified because the inner tumor regions can often be considered to be necrotic and do not contribute to the increase in tumor cells any more. We emphasize that the presented method is not intended to be a biologically viable tumor growth model, it is rather considered to be a fast and simple, but biomechanically justified technique to introduce tumor-induced deformations into an atlas image. This serves as an initialization for non-rigid registration, which offers the possibility to perform atlas-based segmentation of pathologic brain images.

Material properties of brain tissues are taken from Clatz et al. [7] who report a value of 694 Pa for both grey matter and white matter. The fluids were chosen to have a Young's modulus of 0.001 Pa. The skull is assumed to be rigid, while a Young's modulus of 10000 Pa is set for the outward pushing tumor.

### C. The Complete Segmentation Pipeline

In a first step, the atlas is registered to the pathologic patient image using an affine registration procedure for a rough alignment of both images. Subsequently the tumor is grown in the atlas from a manually selected seed point within the tumor region to its approximate shape in the patient, which was previously segmented manually. The seed point is positioned near the center of the patient tumor, avoiding areas that contain CSF because tumors cannot originate from fluid areas. Tumor growth is guided by the hierarchical displacement model described in sect. II-A. In order to obtain better results, especially in the skull boundary regions, the manually segmented tumor shape is eroded and tumor growth is stopped when the volume matches the one of the eroded patient tumor. This step is necessary because the patient tumor boundaries can only be roughly delineated in the atlas after the initial affine registration step. Empirically, we found that erosion of the tumor region by 3 voxels yields the best results. The ultimate shape of the tumor and the segmentation of all other brain tissues is obtained using a non-rigid registration step which accounts for the final precise deformation of tumor and surrounding tissues. We use the well-known ITK implementation of the Diffeomorphic Demons [8] registration method by Vercauteren et al. to register the modified atlas to the pathologic patient image. Diffeomorphic Demons has the advantage that it is comparatively fast and produces a realistic and physically justifiable deformation by ensuring the invertibility of the deformation field. This algorithm is applied in a hierarchical way using three levels of hierarchy, which improves robustness and speed. The deformation field is regularized using Gaussian smoothing with a standard deviation of 1 mm. In order to satisfy the requirements of the sum of squared difference metric, which is used by the Demons algorithm, histogram matching of both images is performed before registration.

## III. RESULTS

The SRI24 atlas [9] was chosen as reference. It is a probabilistic average atlas of 24 healthy humans, which is well-

suites for atlas-based registration due to its sharpness. The atlas offers different MRI modalities and a tissue probability label map.

Axial slices of five different cases with a resolution of 240x240 pixels were investigated. In order to have a ground truth, one study was conducted with two simulated brain tumor images provided by UCINIA [10]. These images are taken from the simulated Brainweb database [11] and used with a complex, realistic FEM-based tumor growth model including mass-effect and infiltration in order to yield a realistic ground truth patient tumor image. Three clinical cases were also considered, one glioma from the Harvard SPL tumor database [12] and two from the ContraCancrum brain tumor database [13]. In case of the SPL patient and the ContraCancrum patients, tissue types were manually segmented for comparison purposes. The segmentation was performed on 2D axial slices of the T1 modality of the MRI images. In order to obtain better registration results, manual skull stripping was performed before the segmentation algorithm was applied to the brain image slices.

Figure 2 shows one simulated case, including a checkerboard image of the tissues and the label map. Figures 3 and 4 depict the SPL patient and one patient from the ContraCancrum brain tumor database, respectively. For these cases, the magnitude of the deformation field induced by the tumor growth is also shown. From Figs. 3 and 4 (bottom right) it can be seen, that the deformation was strong in the area of the tumor, but also affected the surrounding tissues. The further away from the tumor seed, the smaller was the impact of the tumor growth and thus the magnitude of the deformation field. This indicates a plausible qualitative approximation of the tumor mass effect.

The results were promising, both from a visual and from a quantitative point of view. The tumor grew to its approximate shape in the patient, displacing the surrounding tissues. The final non-rigid registration ensured a good match of patient and atlas tumor (Fig. 2,3,4 bottom left) and allowed for a good segmentation of the brain tissues in all cases, as can be seen from the checkerboard images (Fig. 2,3,4 bottom center). We also performed a quantitative comparison of the segmentation accuracy using Dice similarity coefficient, which computes the mean overlap of the respective tissues [14]. The results are reported in Table I. The Dice similarity coefficient was only slightly worse compared to values which were reported in studies of healthy brains [14]. It must be taken into account that both simulated images were very noisy, which makes it difficult to achieve a good overlap. Dice coefficient for the CSF is comparatively low because all fluid regions within the brain are considered. Most other publications focus on the ventricles only and neglect small fluid areas in the boundary regions.

For validation purposes, a standard FEM method was applied to grow the tumor and deform the surrounding tissues using the same mechanical parameters with a standard commercial package (Abaqus®). One simulated case was assessed, which took 4.8 min to be processed on a single core of an Intel® 2.33 GHz CPU (3GB RAM) using the MRF

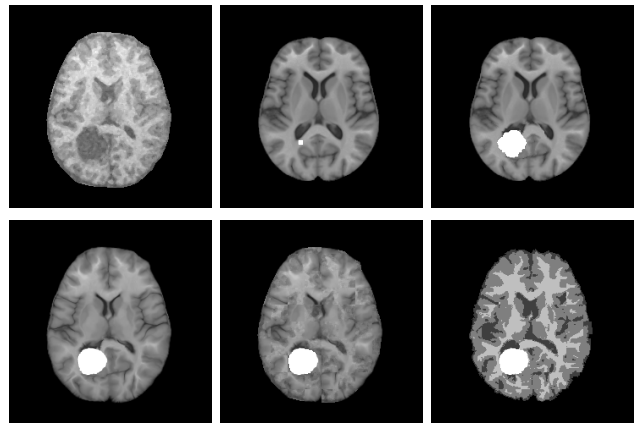


Fig. 2. Results for the simulated tumor case 2. Top row, left to right: Patient image, seeded atlas after affine registration, deformed atlas after tumor growth. Bottom row, left to right: Deformably registered modified atlas, tissue checkerboard of final result, label checkerboard of final result.

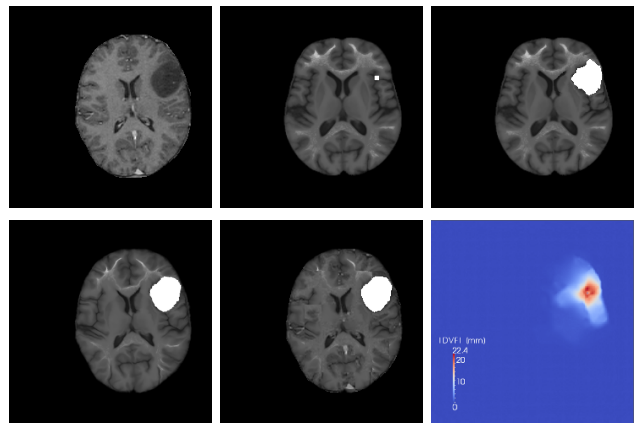


Fig. 3. Results for the SPL patient tumor case. Top row, left to right: Patient image, seeded atlas after affine registration, deformed atlas after tumor growth. Bottom row, left to right: Deformably registered modified atlas, tissue checkerboard of final result, magnitude of the displacement field after tumor growth.

growth method. The mean overlap after non-rigid registration was similar with both approaches while computation time was more than two times higher in case of the FEM method.

## IV. DISCUSSION AND CONCLUSION

### A. Conclusions

We applied a clinically oriented method to deform brain tissues in an atlas in order to be able to perform atlas-based segmentation of brain tumor images. The application to 2D slices serves as a proof of concept for a full 3D implementation of the suggested method. But it can also be useful in a clinical scenario where only few image slices are acquired, which do not constitute a 3D volumetric image. The technique is generally applicable to solid tumors and for simulating the mass-effect of gliomas. Furthermore, it is sufficiently uncomplicated to be used by non-experts in a clinical setting and not only for a limited number of research cases. The technique is based on Markov Random Fields and has the advantage that it does not require any meshing,

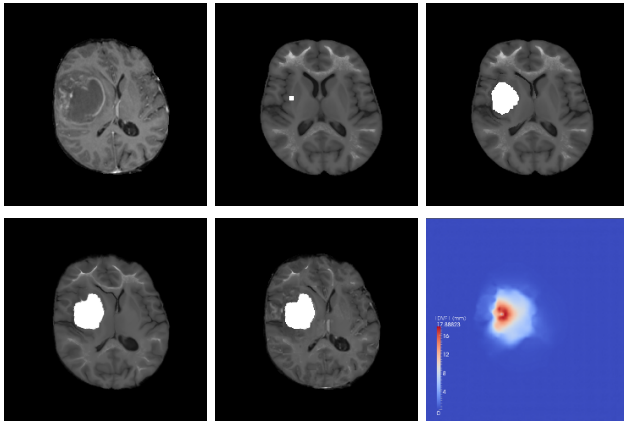


Fig. 4. Results for the ContraCancrum patient tumor case 1. Top row, left to right: Patient image, seeded atlas after affine registration, deformed atlas after tumor growth. Bottom row, left to right: Deformedly registered modified atlas, tissue checkerboard of final result, magnitude of the displacement field after tumor growth.

TABLE I

DICE SIMILARITY COEFFICIENT FOR THE FIVE DATASETS UNDER STUDY.

	CSF	GM	WM	Tumor
Simulated-1	0.48	0.62	0.70	0.95
Simulated-2	0.48	0.63	0.69	0.95
SPL-Patient	0.51	0.62	0.67	0.96
CC-Patient-1	0.40	0.60	0.65	0.96
CC-Patient-2	0.42	0.58	0.60	0.97

in contrast to FEM methods. This offers advantages in a clinical scenario when MR images acquired using a clinical standard protocol have to be processed. The results were analyzed visually and quantitatively against a groundtruth or manual segmentation. The performance of the method was promising and allowed for a good segmentation of brain tissues. Compared to other approaches, this method offers increased robustness and less user interaction thanks to simple parameterization, as well as faster computation time. The only parameters to be selected is the tumor seed location.

### B. Outlook

In contrast to FEM-based methods, this algorithm gives a simpler possibility to introduce a growth displacement field which also considers the final shape of the tumor and not only a circular expansion. This possibility will be further investigated in the future.

The extension of the method to 3D is straightforward and will be done shortly. For the 3-dimensional case, computation time will become an issue, which is why we are planning to parallelize the method on the GPU in 3D. The fact that the MRF approach is only considering a local neighborhood, makes it fairly easy to parallelize the method. In [6] a speed-up factor of up to 60 was reported for 2D cases after implementation on the GPU.

A drawback of the current method is the manual selection of the tumor seed location. Before an automatic seeding method can be implemented, an analysis of the tumor seed location sensitivity has to be undertaken.

## V. ACKNOWLEDGMENTS

Funding by the European Union within the framework of the ContraCancrum project (FP7 – IST-223979) is gratefully acknowledged.

## REFERENCES

- [1] D. Collins, C. Holmes, T. Peters, and A. Evans, "Automatic 3-D model-based neuroanatomical segmentation," *Human Brain Mapping*, vol. 3, pp. 190–208, 1995.
- [2] M. Cuadra, C. Pollo, A. Bardera, O. Cuisenaire, J. Villemure, and J. Thiran, "Atlas-based segmentation of pathological MR brain images using a model of lesion growth," *IEEE Transactions on Medical Imaging*, vol. 23, no. 10, pp. 1301–1314, 2004.
- [3] A. Mohamed, E. Zacharaki, D. Shen, and C. Davatzikos, "Deformable registration of brain tumor images via a statistical model of tumor-induced deformation," *Medical Image Analysis*, vol. 10, no. 5, pp. 752–763, 2006.
- [4] E. Zacharaki, C. Hoge, D. Shen, G. Biros, and C. Davatzikos, "Non-diffeomorphic registration of brain tumor images by simulating tissue loss and tumor growth," *NeuroImage*, vol. 46, no. 3, pp. 762–774, 2009.
- [5] E. Angelini, O. Clatz, E. Mandonnet, E. Konukoglu, L. Capelle, and H. Duffau, "Glioma Dynamics and Computational Models: A Review of Segmentation, Registration, and In Silico Growth Algorithms and their Clinical Applications," *Current Medical Imaging Reviews*, vol. 3, no. 4, pp. 262–276, 2007.
- [6] C. Seiler, P. Buechler, L.-P. Nolte, M. Reyes, and R. Paulsen, "Hierarchical markov random fields applied to model soft tissue deformations on graphics hardware," *Recent Advances in the 3D Physiological Human*, 2009.
- [7] O. Clatz, M. Sermesant, P. Bondiau, H. Delingette, S. Warfield, G. Malandain, and N. Ayache, "Realistic simulation of the 3d growth of brain tumors in mr images coupling diffusion with biomechanical deformation," *IEEE transactions on medical imaging*, vol. 24, no. 10, p. 1334, 2005.
- [8] T. Vercauteren, X. Pennec, A. Perchant, and N. Ayache, "Diffeomorphic demons: Efficient non-parametric image registration," *NeuroImage*, vol. 45, no. 1S1, pp. 61–72, 2009.
- [9] T. Rohlfing, N. Zahr, E. Sullivan, and A. Pfefferbaum, "The SRI24 multi-channel brain atlas: construction and applications," in *Proceedings-Society of Photo-Optical Instrumentation Engineers*, vol. 6914. NIH Public Access, 2008, p. 691409.
- [10] M. Prastawa, E. Bullitt, and G. Gerig, "Simulation of brain tumors in MR images for evaluation of segmentation efficacy," *Medical Image Analysis*, vol. 13, no. 2, pp. 297–311, 2009.
- [11] C. Cocosco, V. Kollokian, R. Kwan, and A. Evans, "Brainweb: Online interface to a 3D MRI simulated brain database," *NeuroImage*, vol. 5, no. 4, p. 425, 1997.
- [12] M. Kaus, S. Warfield, A. Nabavi, P. Black, F. Jolesz, and R. Kikinis, "Automated segmentation of MR images of brain tumors," *Radiology*, vol. 218, no. 2, p. 586, 2001.
- [13] K. Marias, V. Sakkalis, A. Roniotis, C. Farmaki, G. Stamatakos, D. Dionysiou, S. Giatili, N. Uzunoglou, N. Graf, R. Bohle, E. Messe, P. Coveney, S. Manos, S. Wan, A. Folarin, S. Nagl, P. Büchler, T. Baryn, M. Reyes, G. Clapworthy, N. Mcfarlane, E. Liu, T. Bily, M. Balek, M. Karasek, V. Bednar, J. Sabczynski, R. Opfer, S. Renisch, and I. Carlsen, "Clinically oriented translational cancer multilevel modeling: The contracancrum project," in *World Congress on Medical Physics and Biomedical Engineering, September 7 - 12, 2009, Munich, Germany*, ser. IFMBE Proceedings, O. Dössel and W. C. Schlegel, Eds., vol. 25/IV. Springer, 2009, pp. 2124–2127.
- [14] A. Klein, J. Andersson, B. Ardekani, J. Ashburner, B. Avants, M. Chiang, G. Christensen, D. Collins, J. Gee, P. Hellier, *et al.*, "Evaluation of 14 nonlinear deformation algorithms applied to human brain MRI registration," *Neuroimage*, vol. 46, no. 3, pp. 786–802, 2009.